Simulation of contrail coverage over the USA missed during the air traffic shutdown

Patrick Minnis[1], Louis Nguyen, Donald P. Garber,
Atmospheric Sciences, NASA Langley Research Center, Hampton, Virginia, USA

David P. Duda
Hampton University, Hampton, Virginia, USA

Rabindra Palikonda, David R. Doelling
AS&M, Inc., Hampton, Virginia, USA

Abstract
European Conference on Aviation, Atmosphere, and Climate
Friedrichschafen at Lake Constance, Germany
June 30 - July 3, 2003

[1] *Corresponding author:* Patrick Minnis, MS 420, NASA Langley Research Center, Hampton, VA, USA 23681.
Email: p.minnis@nasa.gov

Simulation of contrail coverage over the USA missed during the air traffic shutdown

Patrick Minnis[1], Louis Nguyen, Donald P. Garber,
Atmospheric Sciences, NASA Langley Research Center, Hampton, Virginia, USA

David P. Duda
Hampton University, Hampton, Virginia, USA

Rabindra Palikonda, David R. Doelling
AS&M, Inc., Hampton, Virginia, USA

Keywords: contrails, remote sensing, September 11, contrail simulation, air traffic

ABSTRACT: Contrails were simulated for the northeastern USA during the first part of the air traffic shutdown following the 9-11 terrorist attacks. Analysis of military contrails observed during the shutdown provided a baseline set of contrail properties that were employed to tune a contrail prediction scheme using high-resolution numerical weather analyses and normal air traffic flight data. The simulation produced a large area of contrails that started developing around 1000 UTC, 12 September 2001 and peaked in areal coverage of more than 200,000 km^2 around 1800 UTC. The simulation results were used to alter existing infrared satellite images to visualize the area for air traffic conditions. Initial estimates of the contrail radiative forcing are biased low because of improper treatment of different contrails overlapping on the same satellite imager pixels. Improvements were suggested for a more accurate and complete simulation of the contrail properties.

1 INTRODUCTION

Following the tragic events of 11 September 2001, commercial and personal air traffic over the United States of America (USA) was halted for at least 36 hours with resumption of more normal flight activity by 15 September 2001. During the air traffic shutdown, the contrail coverage decreased dramatically. This lack of contrails over the USA was even noticed by astronauts. Analyses of weather data during the shutdown period indicate an anomaly in the diurnal range of surface air temperature that was attributed to the lack of contrails (Travis et al. 2003). Such an anomaly would result from the lack of radiative forcing by contrails and would indicate not only that contrails affect climate but they can also affect the daily weather. To determine if such an anomaly can be realistically attributed to the absence of normal air traffic, it is necessary to accurately estimate the radiative forcing that would have occurred if normal air traffic had occurred.

Normally, it is difficult to determine the radiative forcing by contrails because air traffic is relatively continuous throughout much of the day (Garber et al. 2003). New and old contrails overlap with each other and with natural cirrus clouds making it difficult to determine the evolution and dissipation of individual contrails and their radiative impacts. The air traffic shutdown was essentially complete by 1600 UTC, 11 September 2001. Thus, the air over the USA should have been free almost all cirrus clouds produced by commercial air traffic by ~ 0000 UTC 12 September. A few isolated contrails from military flights developed over the northeastern USA, an area normally crisscrossed by thousands of flights. By analyzing the evolution and decay of those contrails, Minnis et al. (2002) were able to relate the contrail formation to a specific relative humidity range and estimate the properties of the individual contrails during each hour of their lifetimes. Those initial analyses provide the basis for realistically simulating the effects of the missing air traffic. This paper continues that effort by simulating the contrails that would have developed during that fateful day and by providing preliminary estimates of their potential radiative impact.

[1] *Corresponding author:* Patrick Minnis, MS 420, NASA Langley Research Center, Hampton, VA, USA 23681. Email: p.minnis@nasa.gov

2 DATA AND METHODOLOGY

The basic approach taken here is to use the satellite analyses of Minnis et al. (2002) to determine a relative humidity with respect to ice (RHI) for a given meteorological analysis that can serve as threshold for persistent contrail formation. Flight tracks from a normal air traffic day are then used to simulate the flights through the atmosphere as defined by the meteorological analysis. If the RHI at the location of the plane at a given instant exceeds the threshold RHI value (RHI_t) and the temperature is low enough according to the Appleman criteria, then a persistent contrail is defined for that location. Contrail processes such as spreading, advecting, and dissipating are simulated in a relatively crude fashion and their optical properties are estimated as functions of time. Each contrail is geo-located according to its width, length, and height. This information is then used to alter the satellite image for the given time and location. The original and altered infrared (IR, 10.8 μm) satellite images for each hour are then used to compute the contrail longwave radiative forcing (CLRF).

2.1 *Data*

Hourly data from the eighth Geostationary Operational Environmental Satellite (GOES-8) are used in the simulation. These were also used by Minnis et al. (2002) to analyze the isolated contrails. The GOES-8 4-km IR images from 12 September 2001 serve as the primary dataset, while 1-km IR and split window (12 μm) data from the *NOAA* Advanced Very High Resolution Radiometer (AVHRR) and *Terra* Moderate Resolution Spectroradiometer (MODIS) provide supplementary information.

The temperature (T) and humidity fields are specified using an early version of the NOAA Rapid Update Cycle (RUC) analysis that is based on a hybrid-isentropic model (Benjamin et al. 2003). The RUC reanalyses used here have a 25-hPa vertical resolution in the upper troposphere and a 4-km horizontal resolution, and are available at each hour. RHI is computed from the relative humidity with respect to liquid water derived by the model. The RUC RHI output is similar to the radiosonde profiles in the northeastern USA, but differ by as much as ±20% between 8 and 13 km. (Minnis et al. 2002). The RUC tends to smooth the vertical profiles, reducing the humidity at some locations and increasing it at others. The hourly temperatures, winds (V), and relative humidities were assigned to the satellite data taken closest in time.

It was assumed that the 12 September air traffic would have been identical to the traffic from the previous Thursday. Thus, the simulation uses linear flight tracks (Garber et al. 2003) from 5 September 2001 that were located within the domain bounded by 33°N, 52°N, 66°W, and 93°W. The position of the flight at a given time was associated with the values of T, RHI, and V of the nearest vertical level and the relevant 40-km RUC box.

2.2 *Simulation process*

To persist, contrails and cirrus require RHI ≥ 100%. Because of negative biases in the relative humidity measured at cold temperatures (Miloshevich et al. 1999), RHI infrequently exceeds 100% in the USA radiosonde record. Furthermore, the RUC model adjusts and smoothes the RHI field so that it differs from the radiosonde measurements. While the older version of the RUC used here (discontinued 18 April 2002) yields RHI > 100% more often than the radiosondes, it is still biased low. Thus, it is necessary to increase the RHI from radiosonde measurements for T < 0°C or set an artificially low value of RHI_t.

The threshold was determined by comparing the RUC RHI fields to satellite images of contrail and cirrus distributions using the RUC level having the greatest RHI values in the 150-350 hPa range. Figure 1 shows an example of contrails forming in heavy air traffic over the northeastern USA during 18 November 2001. The leading line of contrails in the *Terra* MODIS 11-12 μm brightness temperature difference image is located in east central Pennsylvania and New York (Fig. 1a). Contrails and cirrus cover most of the image west of that line. Comparison of the 225-hPa RHI contours (Fig. 1b) with the contrails indicate that few contrails formed over areas with RHI < 80%. This value is slightly less than the 85% found by Duda et al. (2003) for a different day. Comparison of the isolated contrails from 12 September yield a different threshold as expected since the RUC alters the humidity field from the measured values as noted earlier. Figure 2a shows a single, but broken linear contrail over Ohio and Pennsylvania at 1108 UTC, 12 September 2001. Cirrus clouds are evident in northern and southern Ohio as well as northeastern Pennsylvania. The contrail pressure was

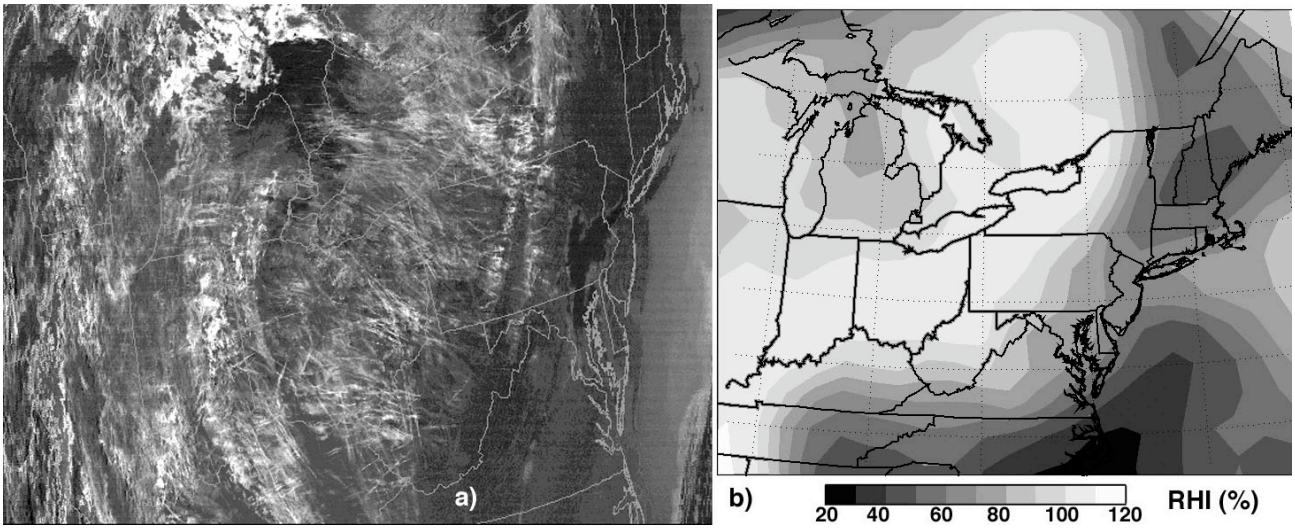

Figure 1. Contrails and humidity over northeastern USA, 18 November 2001. (a) Terra MODIS T11-T12 image, 1624 UTC. (b) 225-hPa RHI (%) from RUC reanalysis, 1600 UTC.

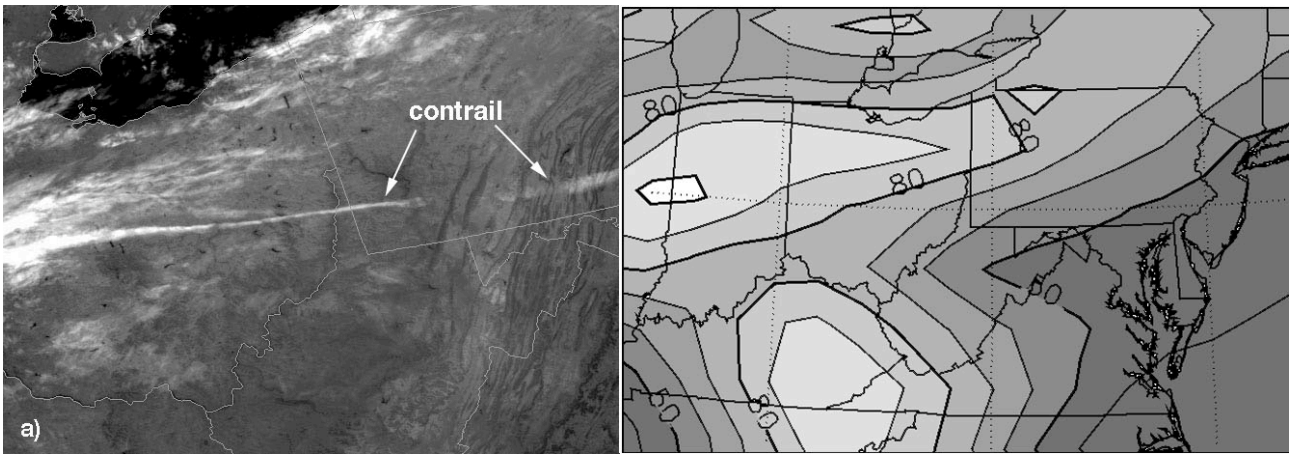

Figure 2. Extended contrail and humidity over northeastern USA, 12 September 2001. (a) NOAA-14 IR image, 1108 UTC. (b) RUC RHI (%) at 225 hPa, 1100 UTC; RHI < 50% in darkest areas.

found to be closest to 225 hPa (Minnis et al. 2002). The corresponding RUC analysis (Fig. 2b) shows that the cirrus occurred for RHI > 80% while the contrail was persisting in air with RHI as low as 58%. Correction of the 1200-UTC local radiosonde data using the Miloshevich et al. (2001) formula indicate that the actual RHI in the domain is probably 30-40% greater than indicated by the RUC (Minnis et al. 2002). Thus, the actual RHI values could exceed 140% in portions (e.g., central Indiana) of domain and should be close to 110% in southeastern Pennsylvania. Comparisons of images and RUC analyses like those in Figure 2 for the remainder of the day led to the conclusion that $RHI_t = 70\%$ for 12 September.

Once formed, the contrails were allowed to spread based on wind shear. It was assumed that the contrails precipitated with a fall speed of 3 cm s^{-1}. This fall speed produced a spreading rate of 6 km h^{-1}, the same as that determined for the isolated military contrails. Although the isolated contrails spread to widths as large as 40 km, it was assumed that the maximum width would be 12 km because it corresponds to the length-weighted average width of the military contrails. No new nucleation was allowed so that the optical mass (*OM*) remained constant as the product of the optical depth (*OD*) and the width once the *OD* reached it peak according to the log-normal function,

$$OM = a \exp\{-0.5 [\ln(x / x_o) / b]^2\}, \quad (1)$$

where x is the mean contrail age, x_o is the time of peak *OM* (2.5 hours), a is peak contrail OM = 0.6, b is the width of the peak (0.5). This function mimics the average behavior of the isolated contrails in the same domain. The contrails are then advected each hour using the winds at the contrail altitude. In the new time step, the contrail is compared to the RHI at its new location. If RHI < 70% in

the RUC box, the portion of the contrail within the box is deleted. It is also deleted if it is over 6 hours old to ensure that the average contrail lifetime is the same as that for the isolated contrails. The endpoints, width, and *OD* of each contrail are saved each hour.

The calculation of CLRF was accomplished in the following manner. The parameters for each contrail at a given hour were used to compute changes to the 4-km GOES-8 IR image by altering the brightness temperature T_{IR} of each pixel affected by the simulated contrail. Figure 3 shows a schematic drawing of four 4-km pixels divided into sixteen 1-km sub-pixels. The fractional contrail coverage in each 4-km pixel is simply the number of 1-km sub-pixels with centers between the lines defining the boundaries of the contrails based on the contrail endpoints and width. In Figure 3, pixel A has a fractional coverage $f_c = 9/16$ compared to 6/16 for pixel D. The contrail optical depth for overlapped sub-pixels is simply the sum of the optical depths for the overlapping contrails. In Figure 3, $OD(\mathrm{B}) = [13*OD(2) + 8*OD(1)] / 15$, while $OD(\mathrm{C}) = 14*OD(1) / 14$. This formulation yields a value that can exceed the pixel contrail optical depth because it includes only portions of the pixel that contain contrails. But it maintains the true OD of the contrails in the pixels. As seen in the schematic drawing, a contrail may be less than 4-km wide, but it can affect two 4-km pixels. To obtain the effective optical depth of the contrails in the pixels, the pixel OD is multiplied by f_c. In the current simulation, however, the OD for each overlap pixel was computed using only the value of OD corresponding to the last contrail that affected the pixel resulting in an underestimate of OD for the pixel.

The new brightness temperature of a given contrail pixel is

$$TC_{IR} = B^{-1}\{[1 - \varepsilon(OD\, f_c)]\, B(T_{IR}) + \varepsilon(OD\, f_c)\, B(TC)\}, \qquad (2)$$

where the emissivity ε is computed using the formula of Minnis et al. (1993) for an axi-symmetrical hexagonal ice column with a length of 20 μm, B is the 10.8-μm Planck function, and TC is the contrail temperature. For this simulation TC is the temperature at 225 hPa. The longwave (5 - 100 μm) fluxes with (M_{LW}) and without (MC_{LW}) contrails is computed as in Minnis and Smith (1998) using a new set of coefficients based on broadband data from the Clouds and Earth's Radiant Energy System scanners. The narrowband IR fluxes (M_{IR}) were computed from the GOES-8 IR brightness temperatures as in Minnis and Smith (1998). The new formula,

$$M_{LW} = 69.56 + 5.516\, M_{IR} - 0.0186\, M_{IR}^2 + -0.123\, M_{IR} \ln(h), \qquad (3)$$

where h is the average column-weighted relative humidity (in percent) above the altitude corresponding to T_{IR} in the RUC profile up to 300 hPa. MC_{LW} is also computed from (3) using the contrail flux, MC_{IR}. The contrail radiative forcing is $CLRF = M_{LW} - MC_{LW}$, where the fluxes represent a single pixel or an average of many pixels over a given area.

The simulation process was performed using all GOES-8 pixels in the domain for each hour between 0945 and 2045 UTC.

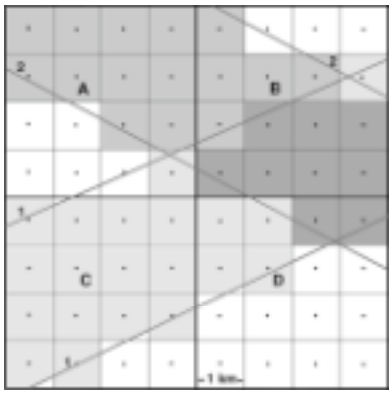

Figure 3. Schematic of method for altering 4-km GOES IR pixels (A - D). Boundaries of contrails 1 and 2 are denoted by the numbered gray lines. 1-km sub-pixels filled by light gray (contrail 1), medium gray (contrail 2), dark gray (overlap).

3 RESULTS & DISCUSSION

Figure 4 shows examples of the original GOES-8 IR images, the contrail masks, and the GOES-IR images containing the simulated contrails for 1045, 1345, 1645, and 1945 UTC. The southern extent of the domain is best represented by the simulated image, but the northern portion is cut off. At 1045 UTC (Fig. 4a), the air traffic for the normal day has just begun over the eastern North America resulting in the generation of a few contrails over South Carolina, western Pennsylvania, and southern Canada. The Canadian contrails are primarily imbedded in extant cirrus and would not be detectable and are cut off in the image. The simulated contrails in northwestern Pennsylvania are similar in appearance to the existing military contrail in southwestern Pennsylvania (Fig. 2 and Fig. 4a3). By 1345 UTC (Fig. 4b), the air traffic is well underway and the contrail coverage is rapidly increasing. The new simulated contrails continue to appear realistic compared to their real counterparts. For example, three military contrails cross West Virginia in an east-west direction while the simulated contrails are oriented north-south. Another east-west contrail in northern Virginia appears to be a continuation of the military contrail in West Virginia. A pronounced mass of overlapping contrails is evident over New Jersey. By 1645 UTC (Fig. 4c), that same mass has moved off the coast and thinned out somewhat (Fig. 4c3). Many new contrails formed while others dissipated. At 1945 UTC (Fig. 4d), many of the contrails have dissipated although the cirrus deck in western Pennsylvania and eastern Ohio has been enhanced considerably by the relatively old contrails that formed in that area. The few spreading contrails over New England appear less realistic than the younger ones, probably as a result of the uniform spreading process used in the simulation. Nevertheless, the resulting imagery, is relatively realistic overall in terms of appearance and compared to the actual contrails that were present.

The total contrail coverage and CLRF for the domain are plotted in Figure 5. The contrail coverage is based on the sum of f_c for the domain divided by total number of pixels, 307,200. The CLRF, however, is based on TC_{IR}, which was computed using the *OD* for only one of the contrails in the overlapped cases and not the sum of the two. The resulting value is, therefore, an underestimate of the CLRF. Contrail coverage (Fig. 5a) peaked at 1745 UTC with a value of 3.66% or slightly more than 200,000 km^2. This result is comparable to the average global linear contrail coverage estimated to be between 200,000 and 400,000 km^2. The total area covered by individual contrails (counting overlapped sub-pixels more than once) peaked at 1745 UTC with 8.85%, 2.4 times more than the actual number of pixels that would be identified as contrail pixels. Thus, overlapped pixels play a critical role in the climatic impact of contrails and need to be treated carefully. Because the mean *OD* was computed only for the individual contrails, it is underestimated. It peaked at a value of 0.257 at 1245 UTC and slowly dropped to 0.138 by 1945 UTC. The *OD*s should be roughly 2.5 times the values found here because of the impact of contrail overlap.

The unit CLRF (Fig. 5b) rises from a negligible value at 0945 UTC to a relatively broad maximum of ~6 Wm^{-2} between 1245 and 1545 UTC. This maximum and the gradual decrease is mostly governed by the variation in *OD*. The total CLRF (contrail forcing relative to the entire domain) is dominated by the contrail coverage and rises to a maximum of 0.25 Wm^{-2} between 1745 and 1845 UTC. The unit CLRF values are 2 - 4 times less than those found by Palikonda et al. (2003) from satellite observations of actual contrails. Some of the difference is due to the co-occurrence of the contrails with cirrus clouds, but the great portion of the difference is most likely due to the underestimate of contrail *OD* for the overlapped pixels. If the *OD*s were increased by 250%, then the unit CLRF would peak at 15.2 Wm^{-2}, a value closer to the daytime September 2001 mean for the linear contrails as derived from AVHRR data (Palikonda et al. 2003). Similarly, the maximum CLRF would be around 0.63 Wm^{-2}. Thus, more realistic values for the simulation can be obtained by multiplying those in Figure 5b by 2.5.

The simulation presented here represents the first step in theoretically evaluating the possible impact of contrails on the daily surface temperature and for explicitly representing contrails in mesoscale weather predictions. A number of improvements and additions are needed to complete the simulation. These include the proper assignment of optical depth for overlapped pixels, more realistic spreading and dissipation schemes, and computation of the shortwave radiative forcing. This latter factor has a more direct and immediate impact on the surface temperature and should act to reduce the maximum daytime temperature more than the CLRF increases it. More detailed radiative transfer modelling will be needed for accurately estimating the shortwave component of the ra-

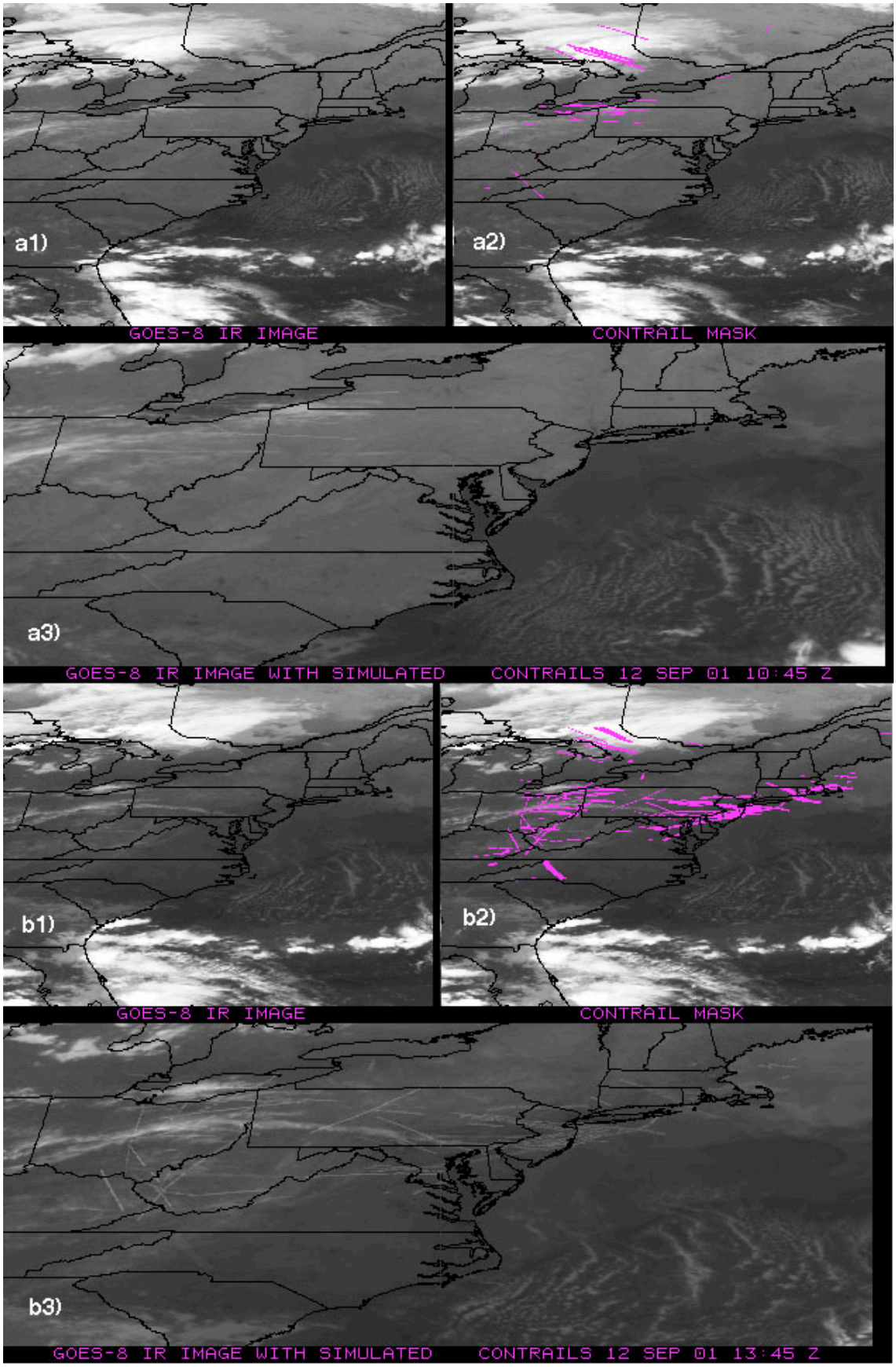

Figure 4. Simulated contrails for 12 September 2001 over northeastern USA. (a) 1045 UTC, (b) 1345 UTC. (1) GOES-8 IR image, (2) IR image with locations of simulated contrails, (3) IR image with simulated contrail IR brightness temperature.

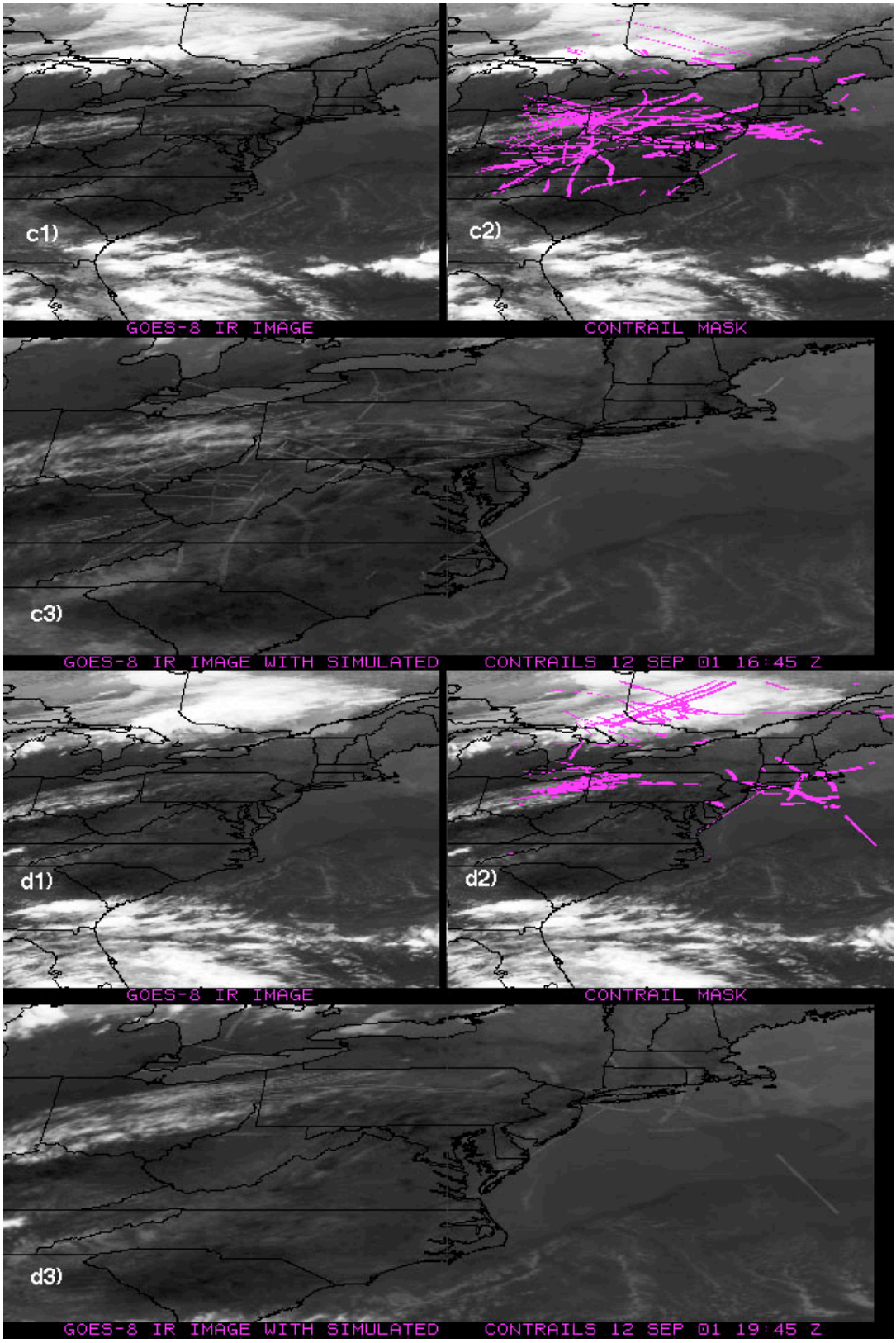

Figure 4 continued. (c) 1645 UTC and (d) 1945 UTC.

diation effect. The radiative forcing will then need to be translated into changes in the surface air temperatures over the region to determine of the magnitude of the anomalies reported by Travis et al. (2003) can be realistically attributed to the absence of contrails during the shutdown. Additional improvements to the simulation should account for variations in contrail optical depths and dissipation rates in order to make the contrails more realistic.

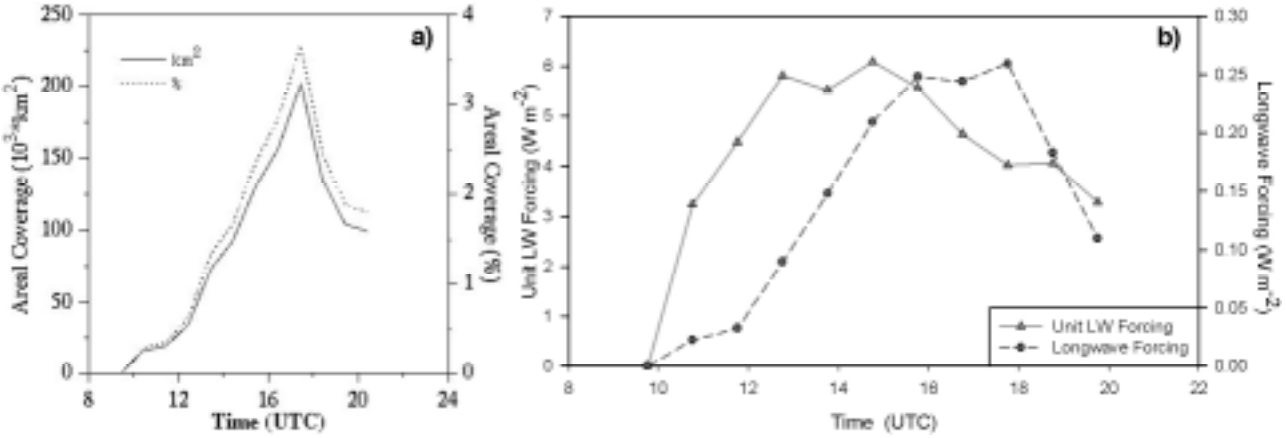

Figure 5. Simulated contrail effects over northeastern USA, 12 September 2001. (a) contrail coverage. (b) contrail longwave radiative forcing.

4 CONCLUDING REMARKS

This initial simulation during the air traffic shutdown, in general, appears to produce realistic contrails. They form in areas where the military contrails persist and are similar in appearance. They also dissipate in areas free of natural cirrus clouds. The analysis confirms the existence of large areas of clear, ice-supersaturated air that are available for additional cirrus formation. The simulations demonstrate that a huge area of contrails would have formed over the northeastern USA if air traffic was normal. This result may help explain of the temperature anomaly found over the same area. With the projected improvements, this simulation should help improve the prediction of contrail formation conditions and contrail lifetimes, and eventually aid the development of reliable predictions of future air traffic effects.

REFERENCES

Benjamin, S. A., G. A. Grell, J. M. Brown, T. G. Smirnova, and R. Bleck, 2003: Mesoscale weather prediction with the RUC hybrid isentropic / terrain-following coordinate model. *Mon Wea. Rev.*, accepted.

Duda, D. P., P. Minnis, P. K. Costulis, and R. Palikonda, 2003: CONUS contrail frequency estimated from RUC and flight track data. *Proc. European Conf. Aviation, Atmosphere, and Climate*, Friedrichshafen at Lake Constance, Germany, June 30 - July 3.

Duda, D. P., P. Minnis, L. Nguyen, and R. Palikonda, 2003: A case study of contrail evolution over the Great Lakes. *J. Atmos. Sci.,* In press.

Garber, D. P., P. Minnis, and P. K. Costulis, 2003: A USA commercial flight track database for upper tropospheric aircraft emission studies. *Proc. European Conf. Aviation, Atmosphere, and Climate*, Friedrichshafen at Lake Constance, Germany, June 30 - July 3.

Miloshevich, L. M., H. Vömel, A. Paukkunen, A. J. Heymsfield, and S. J. Oltmans, 2001: Characterization and correction of relative humidity measurements from Vaisala RS80-A radiosondes at cold temperatures. *J. Atmos. Oceanic Technol.* **18,** 135-156.

Minnis, P. and W. L. Smith, Jr., 1998: Cloud and radiative fields derived from GOES-8 during SUCCESS and the ARM-UAV Spring 1996 Flight Series. *Geophys. Res. Lett.*, **25**, 1113-1116.

Minnis, P., Y. Takano, and K.-N. Liou, 1993: Inference of cirrus cloud properties using satellite-observed visible and infrared radiances, Part I: Parameterization of radiance fields. *J. Atmos. Sci.*, **50**, 1279-1304.

Minnis, P., L. Nguyen, D. P. Duda, and R. Palikonda, 2002: Spreading of isolated contrails during the 2001 air traffic shutdown. *10th AMS Conf. Aviation, range, and Aerospace Meteorol.*, Portland, OR, May 13-16, 33-36.

Palikonda, R., D. N. Phan, V. Chakrapani, and P. Minnis, 2003: Contrail coverage over the USA from MODIS and AVHRR data. *Proc. European Conf. Aviation, Atmosphere, and Climate*, Friedrichshafen at Lake Constance, Germany, June 30 - July 3.

Travis, D., A. Carleton, and R. Lauritsen, 2002: Contrails reduce daily temperature range. *Nature*, **418**, 601.